J|A|C|S
COMMUNICATIONS

Published on Web 10/07/2006

Synthesis and Characterization of $Ge_2Sb_2Te_5$ Nanowires with Memory Switching Effect

Yeonwoong Jung, Se-Ho Lee, Dong-Kyun Ko, and Ritesh Agarwal*

Department of Materials Science and Engineering, University of Pennsylvania, Philadelphia, Pennsylvania 19104

Received August 15, 2006; E-mail: riteshag@seas.upenn.edu

Chalcogenide materials (Ge-Sb-Te alloys) are being widely used for electronic and optical data storage because of their thermally induced, reversible crystalline-to-amorphous phase transition behavior.[1−8] Among many ternary Ge-Sb-Te systems of various chemical compositions, $Ge_2Sb_2Te_5$, in particular, is very promising for nonvolatile memory applications because of the following reasons: (a) extremely fast crystallization rates (<100 ns), (b) high thermal stability at room temperature, and (c) fully reversible amorphous to crystalline phase transition.[1−6,9,10] Therefore, phase transition random access memory (PRAM) utilizing $Ge_2Sb_2Te_5$ have great potential to obviate many intrinsic limitations of conventional memory devices.[11,12] The memory switching effect can be achieved by pulsed electric fields to induce local Joule heating in $Ge_2Sb_2Te_5$ structures, leading to the reversible phase transition.[9,10,13]

However, to achieve high-density memory devices, it is essential to reduce the size of the $Ge_2Sb_2Te_5$ cells to sublithographic length scales, a major bottleneck for achieving the true potential of these materials. The scaling-down of the $Ge_2Sb_2Te_5$ cell is also critical in reducing the current required to amorphize $Ge_2Sb_2Te_5$ (RESET current) rapidly, with less power consumption, thereby enabling fast memory switching speed with high reliability.[9,10,13] The bottom-up approach of assembling nanostructures is a promising solution for scaling down the size of devices. Nanowires (NWs), in particular, can be a powerful approach to assemble memory devices at small length scales, owing to their sublithographic size and unique geometry, which allow device functionality and interconnect to be assembled from the same structure. Recently GeTe and SbTe NWs have been synthesized using single compound precursors;[14,15] however, more complex and technologically significant Ge-Sb-Te ternary NWs and their critical memory switching behavior have not been reported. Here we report the synthesis of ternary $Ge_2Sb_2Te_5$ NWs with control over their chemical composition and demonstrate their feasibility for memory switching. The synthesis of phase-change NWs is also expected to enable critical studies of size-dependent phase transition mechanism at the nanoscale.

$Ge_2Sb_2Te_5$ NWs were synthesized by the vapor transport method via the metal catalyst-mediated vapor-liquid-solid (VLS) mechanism in a horizontal tube furnace.[14−18] Bulk GeTe, Sb, and Te powders (99.99%, Sigma-Aldrich) were used to serve as precursors. On the basis of the melting temperatures of GeTe, Sb, and Te (723, 630, and 449 °C, respectively[19]), and the temperature profile of our tube furnace, the spatial location of the precursors was determined to produce reactants in vapor phase in order to synthesize NWs of the desired composition. GeTe powder was placed at the center of the heating zone while the Te and Sb powders were located separately, seven and three inches apart from the GeTe powder, respectively, at the upstream side of the furnace. The furnace was then slowly heated to 650 °C and maintained for ~2 h. At the downstream side of the furnace, a Si (100) substrate (at a temperature of ~520 °C) covered with Au nanocolloids (diameter ~50 nm) was placed. The vapor phase reactants carried by Ar gas at a flow rate of 200 sccm (base pressure, 50 Torr) condensed on the substrate to produce NWs.

The structure of the NWs was characterized using scanning electron microscopy (SEM) (Figure 1a). The diameters of the NWs range from 20 to 200 nm with lengths up to over 100 μm. The chemical compositions of individual NWs were studied by energy-dispersive X-ray spectroscopy (EDS) in scanning transmission electron microscopy (STEM) using a 1.0 nm-sized probe. The elemental mapping image of the NW (Figure 1b) clearly shows that Ge, Sb, and Te elements are uniformly distributed over the whole NW. Quantitative analysis by EDS point scanning confirms that Ge, Sb, and Te are present in an atomic ratio of 2.02:1.88:5.13. Examination of a large number of NWs revealed that the chemical compositions of the NWs were close to $Ge_2Sb_2Te_5$. In addition, by changing the spatial location of the precursors in the furnace, NWs with various chemical compositions, such as $Ge_1Sb_4Te_7$ and $Ge_1Sb_2Te_4$, were also obtained. Growth at a furnace temperature over 750 °C yielded Te poor NWs with $Ge_3Sb_2Te_3$ composition. These results suggest that the chemical compositions of ternary Ge-Sb-Te NWs can be controlled by varying the location of precursors and growth temperature, although the interplay of these factors in determining the final NW composition needs further elucidation.

The TEM image of $Ge_2Sb_2Te_5$ NWs (Figure 1d) typically shows a nanoparticle attached at the NW end. EDS study confirmed that the particle is composed of Au, suggesting that the NW growth was based on VLS mechanism. A high-resolution TEM (HRTEM) image reveals that the as-synthesized $Ge_2Sb_2Te_5$ NWs are single crystalline (Figure 1d, top inset). The reciprocal lattice peaks obtained by two-dimensional Fourier transform of the HRTEM image (Figure 1d, bottom inset) was indexed to the hexagonal close packed (hcp) $Ge_2Sb_2Te_5$ structure along the (001) zone axis. The hcp structure of the NW is consistent with previous studies of $Ge_2Sb_2Te_5$ thin films,[6,20−22] and is also predicted by the high stability of hcp phase. Typically, in $Ge_2Sb_2Te_5$ thin films, the transition from the amorphous to face-centered cubic (fcc) phase occurs in the temperature range of 100−150 °C and the transition from the fcc to the stable hcp phase occurs in the range of 250−300 °C,[5,6,20−22] which was lower than our growth temperature. The indexed reciprocal lattices show that the growth direction of the NW is along the [110] direction. The measured distances between two adjacent lattice planes was 0.212 nm, corresponding to (110) lattice plane of $Ge_2Sb_2Te_5$ hcp structure with a lattice constant $a = 0.424$ nm.[6,20−22]

The phase transition-based memory switching behavior of $Ge_2Sb_2Te_5$ NWs was studied by electrical measurements. The device characteristics were investigated by measuring the current (I)−voltage (V) curve and resistance (R) change of $Ge_2Sb_2Te_5$ NW-based devices. The NW devices were fabricated by transferring

10.1021/ja065938s CCC: $33.50 © 2006 American Chemical Society

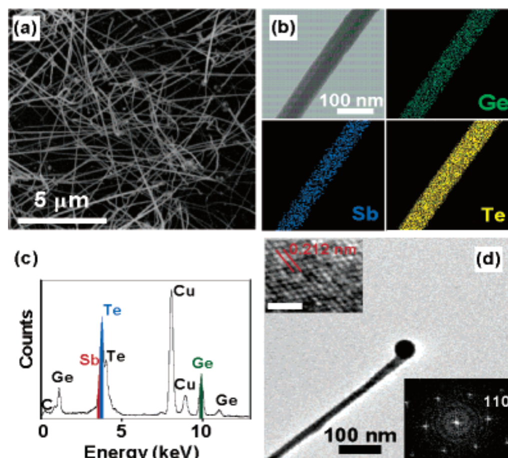

Figure 1. (a) SEM of $Ge_2Sb_2Te_5$ NWs grown on Si substrate; (b) bright field STEM and elemental mapping images of a $Ge_2Sb_2Te_5$ NW; (c) EDS profile of the NW shown in panel b. Cu peaks originate from the TEM grid; (d) TEM and HRTEM images of $Ge_2Sb_2Te_5$ NW and two-dimensional Fourier transform of the HRTEM image: scale bar; 1 nm.

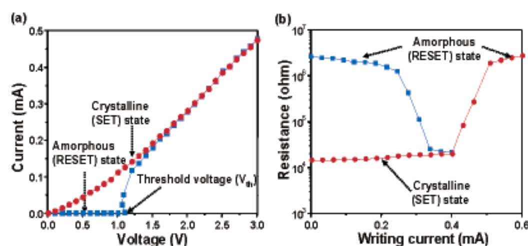

Figure 2. (a) $I-V$ characteristics of a 90 nm diameter crystalline $Ge_2Sb_2Te_5$ NW device (red circles). The $I-V$ characteristics of the NW after applying a current pulse (0.6 mA, 100 ns) that leads to amorphization is shown as blue squares. (b) $R-I$ characteristics of the $Ge_2Sb_2Te_5$ NW device as a function of applied current pulses with varying amplitudes; starting from the crystalline SET state (red circles) and then from the amorphous RESET state (blue squares).

as-synthesized NWs to an oxidized Si substrate, and focused ion beam (FIB) technique was employed to directly write Pt electrodes on the NWs with a separation of 2 μm. Figure 2a is the typical $I-V$ curve of a 90 nm diameter NW (details in Supporting Information). The as-synthesized NW shows ohmic behavior (red circles) with low resistance (7 kΩ), attributed to its original crystalline (SET) state as confirmed by HRTEM. Upon the application of a current pulse (100 ns; 0.6 mA), the NW undergoes memory switching behavior, as signified by the drastic change of the $I-V$ curve (blue squares); the applied current pulse induces crystalline-amorphous phase transition of the $Ge_2Sb_2Te_5$ NW by local Joule heating, while the falling edge of the pulse quenches the $Ge_2Sb_2Te_5$ structure, preventing its recrystallization. At low bias ($<$1.1 V), the $I-V$ curve (blue squares) exhibits a highly resistive amorphous (RESET) state, induced by the current pulse. As the applied voltage reaches a threshold voltage, V_{th}, of 1.1 V, the current rises sharply owing to the recrystallization of the NW (low resistive SET state), thereby recovering its original $I-V$ characteristics. This phenomenon demonstrates that the NW undergoes reversible phase transition from amorphous (RESET) to crystalline (SET) state, as shown in previous studies of $Ge_2Sb_2Te_5$ thin films.[6,8-10,20-22] The NW could be switched reversibly between the RESET and SET states over many cycles (Supporting Information).

Figure 2b shows the variation of the NW resistance upon the application of electrical pulses with varying current amplitudes (called the programming curve), for both crystalline (SET) and amorphous (RESET) states. The dynamic resistance of the NW device which was initially in the SET state increases sharply by over two orders of magnitude when a current pulse (100 ns) above 0.43 mA (red circle) is applied. Meanwhile, the NW which was initially in the RESET state displays a huge decrease in resistance once the current pulse (300 ns) reaches 0.25 mA (blue square). The resistances of RESET and SET states were 2.6×10^6 and 1.8×10^4 Ω, respectively, with the corresponding power consumption of 1.29 and 0.44 mW (Supporting Information). Significantly, the RESET current of 0.43 mA is much lower than the value ($\sim$2.0 mA) currently achieved in commercial PRAM devices utilizing $Ge_2Sb_2Te_5$ thin films.[10]

In conclusion, we have synthesized crystalline ternary $Ge_2Sb_2Te_5$ NWs by the VLS mechanism. The $Ge_2Sb_2Te_5$ NWs are shown to be very promising for next-generation nanoscale memory devices with extremely low power consumption and fast memory switching speeds, with the potential of high-density device integration. Moreover, chalcogenide NWs are expected to open up opportunities to explore the phase transition characteristics of nanostructures, where novel nanoscale phenomena and surface effects will be important.

Acknowledgment. This work is supported by the startup funds from the University of Pennsylvania, and the MRSEC seed award (Grant DMR05-20020).

Supporting Information Available: Detailed explanation of the electrical properties of NWs. This material is available free of charge via the Internet at http://pubs.acs.org.

References

(1) Ovshinsky, S. R. *Phys. Rev. Lett.* **1968**, *21*, 1450−1453.
(2) Adler, D.; Henisch, H. K.; Mott, N. *Rev. Mod. Phys.* **1978**, *50*, 209−220.
(3) Yamada, N.; Ohno, E.; Nishiuchi, K.; Akahira, N. *J. Appl. Phys.* **1991**, *69*, 2849−2856.
(4) Chen, M.; Rubin, K. A.; Barton, R. W. *Appl. Phys. Lett.* **1986**, *49*, 502.
(5) Lankhorst, M. H. R.; Ketelaars, B. W. S. M. M.; Wolters, R. A. M. *Nat. Mater.* **2005**, *4*, 347−352.
(6) Kooi, B. J.; Groot, W. M. G.; Hosson, J. T. M. D. *J. Appl. Phys.* **2004**, *95*, 924−932.
(7) Tsu, D. V. *J. Vac. Sci. Technol. A* **1999**, *17*, 1854.
(8) Lee, B.-S.; Abelson, J. R.; Bishop, S. G.; Kang, D.-H.; Ceong, B.-K.; Kim, K.-B. *J. Appl. Phys.* **2005**, *97*, 093509.
(9) Pirovano, A.; Lacaita, A. L.; Benvenuti, A.; Pellizzer, F.; Bez, R. *IEEE Trans. Electron Devices* **2004**, *51*, 452.
(10) Lee, S.-H.; Hwang, Y. N.; Lee, S. Y.; Ryoo, K. C.; Ahn, S. J.; Koa, H. C.; Jeong, C. W.; Kim, Y.-T.; Koh, G. H.; Jeong, G. T.; Jeong, H. S.; Kim, K. *VLSI Technol. Dig*. **2004**, 20.
(11) Wuttig, M. *Nat. Mater.* **2005**, *4*, 265−266.
(12) Hamann, H. F.; O'Boyle, M.; Martin, Y. C.; Rooks, M.; Wickramasinghe, H. K. *Nat. Mater.* **2006**, *5*, 383−387.
(13) Pirovano, A.; Lacaita, A. L.; Benvenuti, A.; Pellizzer, F.; Hudgens, S.; Bez, R. *IEDM Technol. Dig*. **2003**, 699.
(14) Yu, D.; Wu, J.; Gu, Q.; Park, H. *J. Am. Chem. Soc.* **2006**, *128*, 8148.
(15) Meister, S.; Peng, H.; McIlwrath, K.; Jarausch, K.; Zhang, X. F.; Cui, Y. *Nano Lett.* **2006**, *6* (7), 1514−1517.
(16) Huang, M. H.; Wu, Y.; Feick, H.; Tran, N.; Weber, E.; Yang, P. *Adv. Mater.* **2001**, *13*, 113−116.
(17) Duan, X.; Lieber, C. M. *Adv. Mater.* **2001**, *12*, 298−302.
(18) Wagner, R. S.; Ellis, W. S.; Yashina, *Appl. Phys. Lett.* **1964**, *4*, 89.
(19) http://www.webelements.com/.
(20) Matsunaga, T.; Yamadab, N.; Kubotac, *Y. Acta Crystallogr.* **2004**, *B60*, 685−691.
(21) Sun, Z.; Zhou, J.; Ahuja, R. *Phys. Rev. Lett.* **2006**, *96*, 055507.
(22) Friedrich, I.; Weidenhof, V.; Njoroge. W.; Franz, P.; Wuttig, M. *J. Appl. Phys.* **2000**, *87*, 4130−4134.

JA065938S